Pis'ma v ZhETF, vol. 78, iss. 10, pp. 1167 – 1176

ПО ИТОГАМ ПРОЕКТОВ
РОССИЙСКОГО ФОНДА ФУНДАМЕНТАЛЬНЫХ ИССЛЕДОВАНИЙ
Проекты РФФИ # 00-02-16071а

Nonlinear-laser effects in $\chi^{(3)}$- and $\chi^{(2)}$-active organic single crystals

A. A. Kaminskii[1)]

Institute of Crystallography RAS, 119333 Moscow, Russia

Submitted 9 October 2003

The process of stimulated Raman scattering (SRS) allows to convert laser emission wavelength of crystals providing suitable molecular or lattice mode which contribute to the third order nonlinear optical susceptibility. Renewed interest in this field emerged because of the discovery of SRS in crystals that contain molecular units exhibiting Raman active modes. Particularly, organic nolinear optical crystals used so far frequency doubling and third harmonic generation seem to have a great potential for SRS application. This review paper reported same results on an efficient SRS lasing effects that were discovered recently in organic crystals.

PACS: 42.70.Hj

1. Introduction. Stimulated Raman scattering (SRS) in optical crystalline materials is of topical interest in modern solid-state laser physics. The SRS process allows to shift laser emission wavelength and compress laser pulses, it can improve the spatial quality of laser beams as well as the contrast between peak and background intensities of ultra-short laser pulses, etc. In the last two decides, solid-state SRS science and technology were becoming more wide spread (see, e.g. [1 – 3]). Growth in the activity has been made possible by the discovery of several new SRS-active inorganic crystals, including a successful application given by nano- and picosecond Raman lasers generating specific and otherwise hard to reach wavelengths in a wide spectral range [3 – 5]. Among other current applications of new Raman lasers, remote sensing of the atmosphere is of great interest [6]. Furthermore, crystalline lasers using SRS conversion process are very attractive for medical treatments and for laser guide stars in precise astronomical experiments (see, e.g. [7]).

New generation of Raman lasers requires crystalline materials providing a large frequency shifts up to $3000\,\mathrm{cm}^{-1}$ or more. Unfortunately, with inorganic crystals such shifts are difficult if not impossible to realize due to their ionic structure. As can be seen from Table 1, among known SRS-active inorganic crystals a largest Raman frequency shift has been measured for calcite ($CaCO_3$) [8] and lithium formate monohydrate ($LiHCOO \cdot H_2O$) [9]. During last three years we have been discovered an efficient SRS effects in several organic crystals many of them as indicated in Table 2 possess a frequency shifts as large $3000\,\mathrm{cm}^{-1}$ and a relatively high steady-state Raman gain coefficients for the first Stokes generation. A number of them offer also both nonlinear $\chi^{(3)} + \chi^{(2)}$ susceptibilities, which may give rise to diverse parametric generation acts. It is of interest that in the field of nonlinear optical organic crystals the attention has mainly been directed towards second and third harmonic generation (see, e.g. [25, 26]), but not towards SRS. This is rather astonishing, because the bright optical $\chi^{(3)}$ effect, such as the SRS, was discovered in organic liquid (nitrobenzene) in 60′s just in the beginning of laser era [27].

Present short review represents some main results on SRS spectroscopy of organic crystals - newel family of nonlinear laser solid-state materials, and on new self-frequency conversion parametric effects observed in them under ultra-short laser excitation.

2. The steady-state SRS. The nonlinear frequency conversion effects (SHG, SRS, etc.) are possible in any optically transparent crystals in which the electron cloud of atoms tend to be polarized, i.e. the refractive index n is a function of the electric-field strength $\mathbf{E}$ of the propagating laser emission through these crystals (see, e.g. [28 – 30])

$$n(\mathbf{E}) = n_0 + n_1\mathbf{E} + n_2\mathbf{E}^2 + \ldots \qquad (1)$$

[1)] e-mail: kaminalex@mail.ru

Table 1

Selected easily accessible inorganic SRS-active crystals with laser frequency shift (ω_{SRS}) more than 900 cm^{-1} [2, 3, 5, 8 – 11]*

Crystal	Space group		Nonlinearity (class)	Lagest SRS-active vibration mode (cm^{-1})
	Notation	Number		
$LiHCOO{\cdot}H_2O$	$C_{2v}^9 - Pna2_1$	(No. 33)	$\chi^{(2)} + \chi^{(3)}$ (polar)	≈ 1372
$NaClO_3$	$T^4 - P2_13$	(No. 198)	$\chi^{(2)} + \chi^{(3)}$	≈ 936
$NaY(WO_4)_2$	$C_{4h}^6 - I4_2/a$	(No. 88)	$\chi^{(3)}$	≈ 914
KH_2PO_4 (KDP)	$D_{2d}^{12} - I\bar{4}_22d$	(No. 122)	$\chi^{(2)} + \chi^{(3)}$	≈ 915
$KAl(SO_4)_2 \cdot 12H_2O$	$T_h^6 - Pa3$	(No. 205)	$\chi^{(3)}$	≈ 989
α-$KY(WO_4)_2$	$C_{2h}^6 - C2/c$	(No. 15)	$\chi^{(3)}$	905
α-$KGd(WO_4)_2$	$C_{2h}^6 - C2/c$	(No. 15)	$\chi^{(3)}$	901
α-$KYb(WO_4)_2$	$C_{2h}^6 - C2/c$	(No. 15)	$\chi^{(3)}$	≈ 907
α-$KLu(WO_4)_2$	$C_{2h}^6 - C2/c$	(No. 15)	$\chi^{(3)}$	907
$CaCO_3$	$D_{3d}^6 - R3c$	(No. 167)	$\chi^{(3)}$	≈ 1085
$Ca_4Gd(BO_3)_3O$	$C_s^3 - Cm$	(No. 8)	$\chi^{(2)} + \chi^{(3)}$ (polar)	933
$CaWO_4$	$C_{4h}^6 - I4_2/a$	(No. 88)	$\chi^{(3)}$	≈ 908
$ZnWO_4$	$C_{2h}^4 - P2/c$	(No. 13)	$\chi^{(3)}$	907
$Sr_5(PO_4)_3F$	$C_{6h}^2 - P6_3/m$	(No. 176)	$\chi^{(3)}$	950
$SrWO_4$	$C_{4h}^6 - I4_2/a$	(No. 88)	$\chi^{(3)}$	922
$Ba(NO_3)_2$	$T_h^6 - Pa3$	(No. 205)	$\chi^{(3)}$	≈ 1047
$BaWO_4$	$C_{4h}^6 - I4_2/a$	(No. 88)	$\chi^{(3)}$	924
β'-$Gd_2(MoO_4)_3$	$C_{2v}^8 - Pba2$	(No. 32)	$\chi^{(2)} + \chi^{(3)}$ (polar)	960
$PbWO_4$	$C_{4h}^6 - I4_2/a$	(No. 88)	$\chi^{(3)}$	901

*Most of these crystals are already commercial materials as the laser host-crystals (indicated by bold letters) and crystals for second harmonic generation (SHG), as well as some of them are well known birefringent and scintillator crystals (see, e.g. [12 – 15]). The diamond is also $\chi^{(3)}$-active crystal with $\omega_{SRS} \approx 1333\,\text{cm}^{-1}$ [16], but it is not easily accessible.

here n_0 is the "linear" refractive index, and n_1, n_2 and so on are the higher-order coefficient of $n(\mathbf{E})$. A dielectric polarization vector $\mathbf{P}$, defined as the electric dipole moment of the optical crystal can be described phenomenologically in terms of nonlinear susceptibility tensor of a crystal by expressing its polarization as a power series in electric-field strength $\mathbf{E}$ as

$$\mathbf{P}(\mathbf{E}) = \chi^{(0)}\mathbf{E} + \chi^{(2)}\mathbf{E}^2 + \chi^{(3)}\mathbf{E}^3 + \ldots \qquad (2)$$

where $\chi^{(0)}$ is the linear susceptibility tensor responsible for linear optical phenomena such as refraction and reflection of the light; and $\chi^{(2)}$, $\chi^{(3)}$, etc. are the nonlinear optical susceptibilities of a crystal. These tensors are related to the linear and nonlinear refractive index as follows

$$\chi^{(0)} \cong \frac{1}{4\pi}(n_0^2 - 1), \quad \chi^{(2)} \cong \frac{1}{2\pi}n_0 n_1, \quad \chi^{(3)} \cong \frac{1}{2\pi}n_0 n_2, \qquad (3)$$

and responsible for a large variety of nonlinear optical phenomena. The most important nonlinear frequency conversion effects arise from the second and third terms in Eq. (2), which are connected to electrical polarization as the are quadratic and cubic functions of the electrical field strength. The second terms in Eq. (2) in gives rise to frequency mixing, in particular SHG in acentric crystals, whereas the tensor $\chi^{(3)}$ of the third terms is not subsided to symmetry restrictions. Therefore, in $\chi^{(3)}$-active crystals several nonlinear processes, such as SRS, third harmonic generation and so on are available in optically isotropic and anisotropic crystals (Table 3).

The Raman lasers based on $\chi^{(3)}$-crystals as mentioned above are extensively growing area in modern laser material science and solid-state laser physics. It is not feasible to present an examination of main theoretical aspects of SRS laser frequency conversion in solids used so far. A few such comprehensive reviews are already present in the literature (see, e.g. [1, 3, 28, 29, 31 – 34]). Depending on the pump pulse duration τ_p, two temporal SRS regimes, steady-state and transient, can be considered. The main condition for the steady-state pumping condition, which is of more interested for many practical cases and which was realized in most known nano- and picosecond crystalline Raman lasers, is

$$\tau_p \gg T_2 = (\pi\Delta\nu_R)^{-1}, \qquad (4)$$

Table 2

SRS-active organic and organometallic crystals [17 – 21]

Crystal	Space group		Nonlinearity (class)	SRS-active vibration mode (cm^{-1})	Observed nonlinear laser effect[1)]
	Notation	Number			
Organic					
$C_{12}H_{22}O_{11}$[2)] (sucrose, sugar)	$C_2^2 - P2_1$	(No. 4)	$\chi^{(2)} + \chi^{(3)}$ (polar)	≈ 2960	SHG, SRS, self-FD, self-SFM
$C_{13}H_{10}O$ (benzophenone)	$D_2^4 - P2_12_12_1$	(No. 19)	$\chi^{(2)} + \chi^{(3)}$	3070, 1650, 998, ≈ 103	SHG, SRS
$C_{13}H_{10}O_3$	$D_{2h}^5 - Pbca$	(No. 61)	$\chi^{(3)}$	≈ 3150	SRS
(salol)					
α-$C_{14}H_{12}O$[3)] (4-methylbenzophenone)	$C_{2h}^5 - P2_1/c$	(No.14)	$\chi^{(3)}$	3065	SRS
$C_{14}H_{10}O_2$[4)] (benzil, dibenzoyl)	$D_3^4 - P3_121$	(No.152)	$\chi^{(2)} + \chi^{(3)}$	≈ 1000	SHG, SRS
$C_{15}H_{19}N_3O_2$ (AANP)[5)]	$C_{2v}^9 - Pna2_1$	(No. 33)	$\chi^{(2)} + \chi^{(3)}$ (polar)	≈ 1280	SHG, SRS, self-SFM
$C_{16}H_{15}N_3O_4$ (MNBA)[6)]	$C_s^4 - Cc$	(No. 9)	$\chi^{(2)} + \chi^{(3)}$ (polar)	≈ 1587	SHG, SRS, self-FD, self-SFM
Organometallic					
$C_{14}H_{26}N_8O_{13}Zr$ (GuZN-III)[7)]	$D_2^5 - C222_1$	(No. 20)	$\chi^{(2)} + \chi^{(3)}$	≈ 1008, ≈ 2940	SHG, SRS
$C_{13}H_{22}N_5TlZr$ (TlGuZN)[8)]	$C_2^2 - P2_1$	(No. 4)	$\chi^{(2)} + \chi^{(3)}$ (polar)	≈ 1005, ≈ 2950	SHG, SRS

[1)] Used abbreviations self-FD and self-SFM are the self-frequency doubling and the self-sum-frequency mixing, correspondingly.
[2)] Strongly shifted Stokes and anti-Stokes picosecond generation ($\omega_{SRS} \approx 2915\,cm^{-1}$) was observed also in glassy sugar caramel. Both sugar materials, single crystals and glassy caramel are easily accessible and very cheap. They were bought in pastry shops.
[3)] It is known also the metastable β-$C_{14}H_{12}O$ phase which has trigonal space group $C_3^2 - P3_1$ (No.144) or $C_3^3 - P3_2$ (No.145) [22].
[4)] In accordance with [23] space group could be also $D_3^6 - P3_221$ (No.154).
[5)] Full chemical name is the 2-adamantylamino-5-nitropyridine.
[6)] Full chemical name is the 4′-nitrobenzylidene-3-acetamino-4-methoxyaniline.
[7)] Full chemical name is the bis(guanidinium) zirconium bis(nitrilotriacetate) hydrate.
[8)] Full chemical name is the thallium quanidinium zirconium bis(nitrilotriacetate) dihydrate [24]. Refined data on SRS and SHG will be published soon with Dr. E.Haussühl, who grew and characterized of this crystal.

here T_2 is the dephasing (phonon relaxation) time of the SRS-active vibration mode and $\Delta\nu_R$ is the linewidth (FWHM) of the corresponding Raman-shifted line with a frequency ω_{SRS} in the spontaneous Raman scattering spectrum. The condition for the first Stokes steady-state generation regime in Raman lasers based on $\chi^{(3)}$-active crystals [35]

$$R_m \exp\left[2(g_{ssR}^{St_1} I_p l_{SRS} - \alpha l_{cr})\right]_{\lambda_{St1}} = 1 \qquad (5)$$

is very nearly the same as the condition for stimulated-emission (SE) generation in the usual lasers on the base of activated crystals [36]

$$R_m \exp[2(\Delta N \sigma_{SE} l_{SE} - \rho l_{cr})]_{\lambda_{SE}} = 1. \qquad (6)$$

In Eqs. (5) and (6): $g_{ssR}^{St_1} I_p L_{SRS}$ is the Raman gain factor (here: $g_{ssR}^{St_1}$ is the steady-state Raman gain coefficient, I_p is the laser pumping intensity, and l_{SRS} is the SRS-active crystal length), α is the loss coefficient at the first Stokes wavelength λ_{St_1}, l_{cr} is the total crystal length, $R_m = R_{m1}R_{m2}$ is the reflectivity of resonator mirrors, $\Delta N \sigma_{SE}$ is the gain coefficient (here: ΔN is the inversion population of the Stark laser levels and σ_{SE} is the cross-section of inter-Stark laser transition of an activator ions), and ρ is the loss coefficient at the SE wavelength λ_{SE}.

If the intensity of plane-wave fundamental pump-laser radiation is much higher than the intensity of the first Stokes generation ($I_p \gg I_{St_1}$), i.e. when the level

Table 3

Some possible $\chi^{(2)}$- and $\chi^{(3)}$-effects in undoped nonlinear-laser crystals (see, e.g. [31])

Nonlinear effect[1)]	Frequency		Nonlinear Susceptibility	Note
	Incident	Created		
Second harmonic generation[2)]	ω, ω	2ω	$\chi^{(2)}$	UV and visible generation
Sum frequency mixing[2)]	ω_1, ω_2	$\omega_3 = \omega_1 + \omega_2$	$\chi^{(2)}$	Up-conversion
Difference frequency mixing[2)]	ω_1, ω_2	$\omega_3 = \omega_1 - \omega_2$	$\chi^{(2)}$	IR generation
Third harmonic generation[2)]	ω, ω, ω	3ω	$\chi^{(2)}$	VUV generation
Sum frequency mixing[2)]	$\omega_1, \omega_2, \omega_3$	$\omega_4 = \omega_1 + \omega_2 + \omega_3$		VUV and UV generation
Stimulated Raman scattering[3)]	ω_1	ω_2	$\chi^{(3)}$	$\omega_2 = \omega_1 \pm \omega_{SRS}$
Two-photon absorption[3)]	ω, ω	–	$\chi^{(3)}$	$\omega_c = 2\omega$

[1)] It is available also self-frequency conversion effects, namely self-FD, self-SRS, etc.
[2)] Phase matching required.
[3)] ω_{SRS} and ω_c are the crystal frequencies.

of pump depletion is very small, the SRS amplification at the first Stokes emission can be written [37] as

$$\frac{dI_{St_1}}{d_{SRS}} = g_{ssR}^{St_1} I_p(l_{SRS}) \cdot I_{St_1}(l_{SRS}) + $$

$$+ I_p(l_{SRS}) \cdot \frac{d\sigma}{d\Omega} N_{SRS} \Delta\Omega =$$

$$= g_{ssR}^{St_1} I_p(l_{SRS}) [I_{St_1}(l_{SRS}) + I_{St_1}(l_{SRS} = 0)], \qquad (7)$$

where $I_{St_1}(l_{SRS} = 0)$ is the intensity of the spontaneous Raman scattering at the wavelength λ_{St_1} of the first Stokes generation (in the beginning $l_{SRS} = 0$ of the amplified crystal, i.e. from zero-point fluctuation of spontaneous scattering)

$$g_{ssR}^{St_1} = \frac{2\lambda_{St_1}^2 N_{SRS}}{\pi n_{St_1}^2 h\nu_p} \frac{d\sigma}{d\Omega} \frac{1}{\Delta\nu_R}. \qquad (8)$$

Clearly, in the first Stokes lasing process, very weak spontaneous Stokes Raman scattering provides the major contribution, because its frequency-shifted emission at ω_{SRS} of the intensive line (s) acts as a "seed" for SRS amplification. This situation is analogous to the luminescence (spontaneous emission) in the laser action in activated crystals. In Eqs. (7) and (8): $d\sigma/d\Omega$ is the Raman scattering cross-section of the vibration transition of the crystal, N_{SRS} is the number (concentration) of SRS-active scattering centers n_{St_1}, is the refractive index of the crystal at wavelength λ_{St_1}, and $\Delta\Omega$ is the small solid angle of SRS lasing. As seen from Eq. (8), the $g_{ssR}^{St_1}$ coefficient is linearly proportional to the Raman scattering cross-section and inversely proportional to the linewidth of the spontaneous Raman scattering transition. The product $\frac{d\sigma}{d\Omega} \cdot \frac{1}{\Delta\nu_R}$ may be considered as the spectroscopic parameter providing a measure for peak intensity of a spontaneous Raman transition. This figure of merit, as shown in [38, 39], can be used in a comparative selection for suitable SRS-active crystals. Therefore, high-gain Raman crystals for steady-state SRS laser converters should have a small $\Delta\nu_R$ value and strong spontaneous Raman scattering transition. Solving Eq. (7) yields (see, e.g. [29])

$$I_{St_1}(l_{SRS}) = I_{St_1}(l_{SRS} = 0) \exp(g_{ssR}^{St_1} I_p l_{SRS}). \qquad (9)$$

In many known experimental cases (see, e.g. [3, 30, 32, 33, 40]) SRS lasing at the first Stokes wavelength ($\omega_{St_1} = \omega_p - \omega_{SRS}$) becomes with any assurance measurable when the increment in Eq. (9) reaches a value of $g_{ssR}^{St_1} I_p l_{SRS} = 25$–$30$, which corresponds to a energy conversion efficiency of approximately 1%. The laser pumping intensity ($I_p = I_{thr}$) providing such an efficiency value is conditionally considered as the first Stokes steady-state threshold pumping intensity ($I_{St_1}/I_{thr} \approx 0.01$). Thus approach makes possible tentatively estimate of the $g_{ssR}^{St_1}$ value for $\chi^{(3)}$-active crystals in rather simple pumping geometries, as in the single-pass SRS experiments (see, e.g. [11, 41]).

Due to very strong $\chi^{(3)}$- and $\chi^{(2)}$-nonlinearities of the most used organic crystals (see Table 2), the pumping condition in conducted SRS experiments were slightly different from the model mentioned above. To avoid a manifestation of other possible nonlinear effects (SHG, two-photon absorption and so on) in them, we can make only a comparative estimation of their $g_{ssR}^{St_1}$ coefficients applying several reference $\chi^{(3)}$-active crystals ($PbWO_4$, α-$KY(WO_4)_2$, α-$KGd(WO_4)_2$, and $NaClO_3$ [14, 42, 43]) and relatively "soft" excitation condition.

As a threshold intensity in these comparative experiments we assumed the pumping energy at which the steady-state first Stokes lasing becomes confidently perceptible (usually with signal/noise ratio $\approx$ 2). Conducted measurements with our organic crystals showed that in the most cases their first-Stokes pumping "soft" threshold significantly less then the "1%-threshold".

3. SRS spectroscopy of organic single crystals. The spectroscopic single-pass SRS experiments in [17–21] were done using oriented samples of organic single crystals with different active length (from

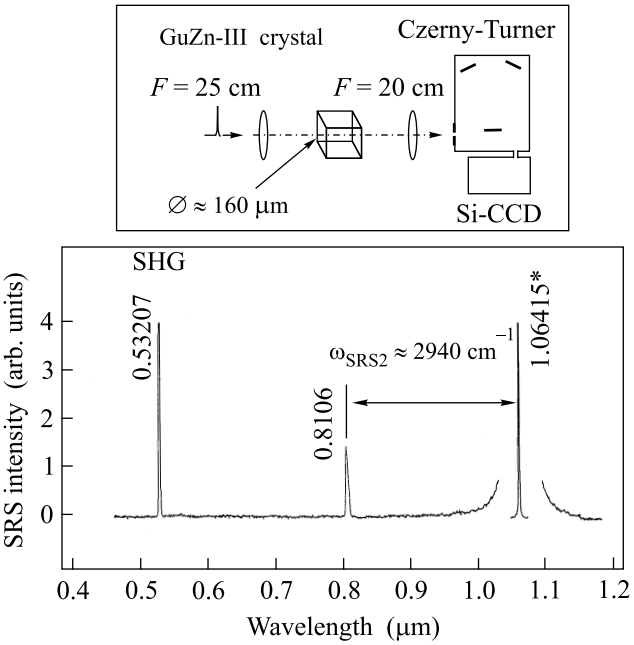

Fig.1 The orientational SRS and SHG spectrum of an orthorhombic $C_{14}H_{26}N_8O_{13}Zr$ (GuZN-III) crystal obtained in pumping geometry $c(aa)c$ under picosecond excitation at $\lambda_{f1} = 1.06415\,\mu$m wavelength (fundamental pump line is asterisked), as well as a scheme of the experimental single-pass set-up (above) [20]. Wavelengths of all lines are given in μm and their intensity are shown without correction of spectral sensitivity of used analyzing CSMA system (see Fig.2). Anti-Stokes line related to SRS-active vibration mode of the crystal $\omega_{SRS2} \approx 2940\,\mathrm{cm}^{-1}$ is indicated by the horizontal arrow

$l_{SRS} \approx 0.5$ mm for AANP to $l_{SRS} \approx 25$ mm for benzophenone and GuZN-III). The reference and measured crystals were equal in length and their optical faces were polished plane-parallel but not anti-reflection coated. For the excitation steady-state Stokes and anti-Stokes generation in organic crystals, we used a homemade picosecond $Nd^{3+}:Y_3Al_5O_{12}$ laser with $\approx 30\%$ efficient frequency doubler that generates ≈ 110 ps pulses (FWHM) at $\lambda_{f1} = 1.06415\,\mu$m and an energy up 3 mJ,

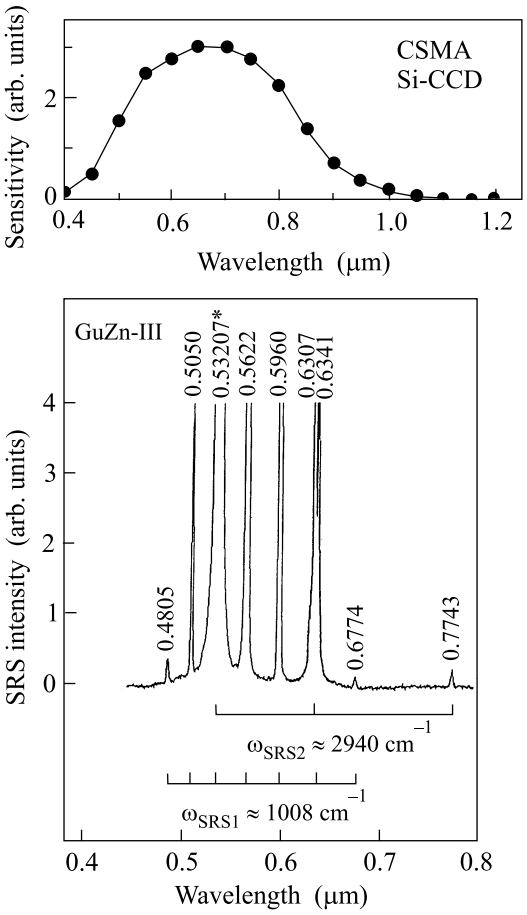

Fig.2. The orientational SRS and RFWM spectrum of an orthorhombic $C_{14}H_{26}N_8O_{13}Zr$ (GuZN-III) crystal obtained in pumping geometry $a(cc)a$ under picosecond excitation at $\lambda_{f2} = 0.53207\,\mu$m wavelength, as well as wavelength dependence the spectral sensitivity of used analyzing CSMA system (above) [20]. Stokes and anti-Stokes lines related to SRS-active vibration modes of the crystal $\omega_{SRS1} \approx 1008\,\mathrm{cm}^{-1}$ and $\omega_{SRS2} \approx 2940\,\mathrm{cm}^{-1}$ are indicated by horizontal brackets. Other notations as in Fig.1

and ≈ 80 ps SHG at $\lambda_{f2} = 0.53207\,\mu$m wavelength [44]. Pump radiation with Gaussian beam profile, as need, were focused onto the investigated crystal by a lens with a focal distance adjusted ($F = 25$ cm) such that the SRS lasing was maximum without a surface and volume optical damage sample, resulting in a beam waist diameter of about 160 μm (see used setup in the frame of Fig.1). The spectral composition of the Stokes and anti-Stokes, as well as self-FD and self SFM generation emission was measured with a CCD-spectroscopic multichannel analyzer (CSMA) consisting of a scanning grating monochromator (with Czerny-Turner arrangement), an analyzer, and a Si-CCD array-sensor (Hamamatsu S3923-1024Q) as a detector. The sensitivity dispersion of this

CSMA system is given in the inset of Fig.2. Below are shown several selected SRS spectra of investigated organic crystals.

3.1. $C_{14}H_{22}N_8O_{13}Zr$ (GuZN-III) crystal [20], two SRS-spectra (see Fig.1 and 2) are shown an identification of observed Stokes and anti-Stokes lines related to two SRS-active optical vibration modes of the crystal $\omega_{SRS1} \approx 1008\,\mathrm{cm}^{-1}$ and $\omega_{SRS2} \approx 2940\,\mathrm{cm}^{-1}$. The analysis is shown that for the 62-atomic molecule $C_{14}H_{26}N_8O_{13}Zr$ of a GuZN-III structure with orthorhombic space group D_2^5 and $Z = 4$ (2 for primitive unit cell) overall degrees of freedom $(3N \times 2) = 372$ distributed into (at $\mathbf{k} = 0$, center of Brillouin zone):

$$\Gamma_N = 92A + 94B_1 + 93B_2 + 93B_3$$

irreducible representations. In accordance with [45], the A modes of a GuZN-III crystal are Raman active only, and those of B_1, B_2, and B_3 are both Raman and IR active. Among them the $(B_1 + B_2 + B_3)$ species are acoustic modes. As an illustration, Fig.3 shows the Raman spectrum of the fully symmetric A species, which

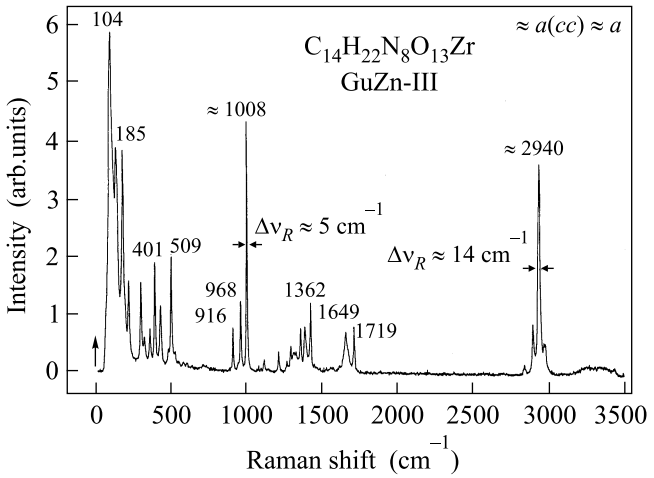

Fig.3. The room-temperature polarized spontaneous Raman scattering spectrum of an orthorhombic $C_{14}H_{26}N_8O_{13}Zr$ (GuZN-III) crystal registered under experimental geometry $\approx a(cc) \approx a$ [20]. Raman shift of several intensive lines are given in cm^{-1}. The arrow at zero corresponds to excitation by CW $Nd^{3+} : Y_3Al_5O_{12}$ laser at 1.06415 μm wavelength

was recorded under excitation geometry $\approx a(cc) \approx a$ practically as in the case of the SRS spectrum exhibited in Fig.2. The assignment of its strongest Raman shifted lines to the respective vibration modes of a GuZN-III crystal yields that the A-symmetry lines at ≈ 1008 and $\approx 2940\,\mathrm{cm}^{-1}$ are promoting modes of observed SRS lasing components. They correspond to the stretching vibrations of the CH_2 and N-C-O bond systems, respectively.

3.2. $C_{13}H_{10}O$ (benzophenone), **α-$C_{14}H_{12}O$** (4-methylbenzophenone), and **$C_{14}H_{10}O_2$** (benzil) crystals [18]. Their Stokes and anti-Stokes spectra are given in Figs.4 and 5. The analysis conducted

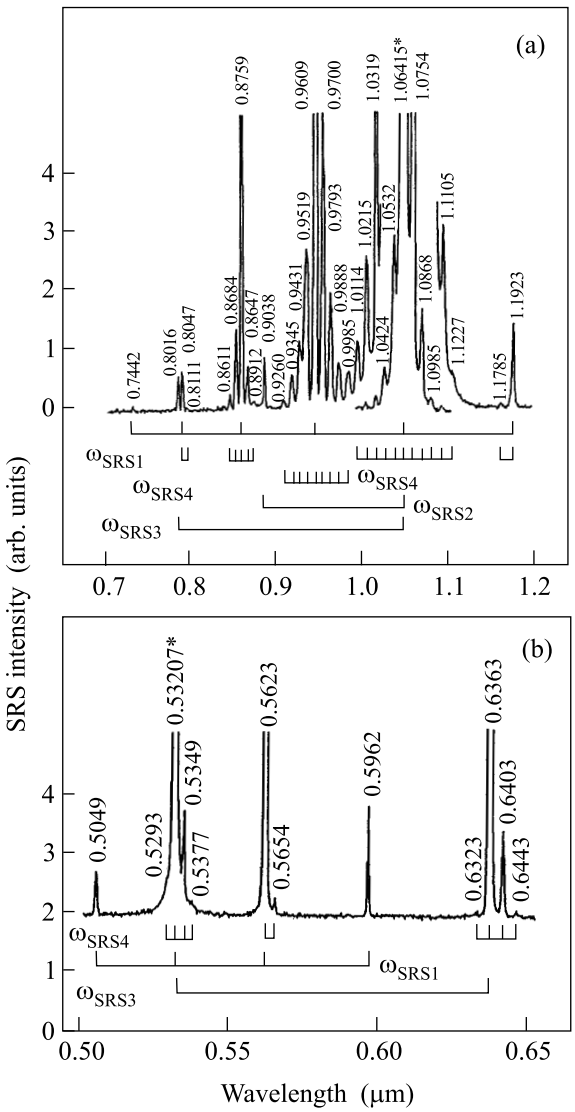

Fig.4. The orientational SRS and RFWM spectra of an orthorhombic $C_{13}H_{10}O$ (benzophenone) crystal obtained in pumping geometry $\approx b(\approx c \approx c) \approx b$ under picosecond excitation at (a) $\lambda_{f1} = 1.06415\,\mu$m and (b) $\lambda_{f2} = 0.53207\,\mu$m wavelengths [18]. Stokes and anti-Stokes lasing lines related to SRS-active vibration modes of the crystals $\omega_{SRS1} = 998\,\mathrm{cm}^{-1}$, $\omega_{SRS2} = 1650\,\mathrm{cm}^{-1}$, $\omega_{SRS3} = 3070\,\mathrm{cm}^{-1}$, and $\omega_{SRS4} \approx 103\,\mathrm{cm}^{-1}$ are indicated by horizontal brackets. Other notations as in Fig.1

in [18] is shown that most of their SRS-active modes (with the frequency of ≈ 3070, 1650, and $\approx 1000\,\mathrm{cm}^{-1}$)

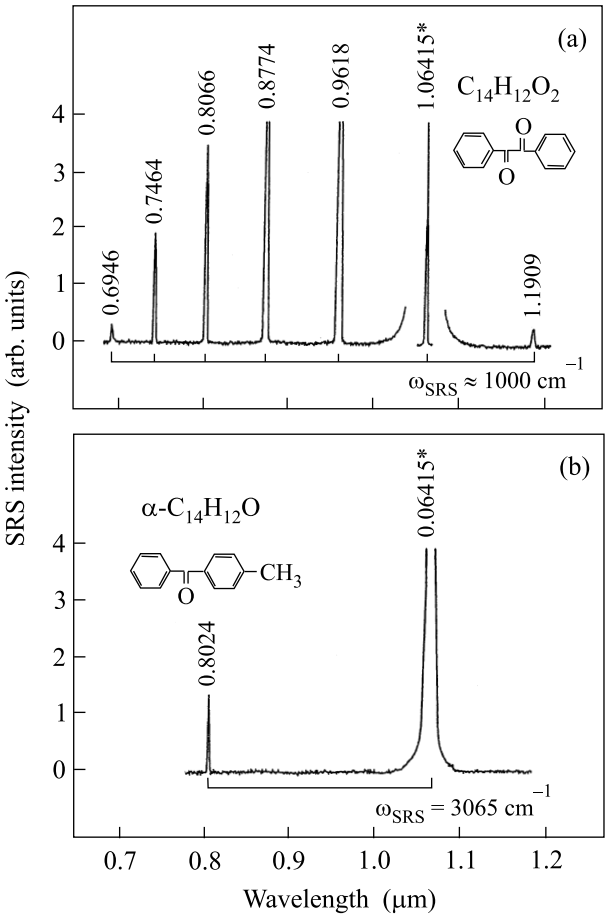

Fig.5. Stokes and anti-Stokes lasing spectra of (a) a trigonal $C_{14}H_{10}O_2$ (benzil) and (b) a monoclinic α-$C_{14}H_{12}O$ (4-methylbenzophenone) crystals obtained under picosecond excitation at $\lambda_{f1} = 1.06415$ μm wavelength [18]. Pumping geometry for $C_{14}H_{10}O_2$ crystal was $\perp b (\approx b \approx b) \perp b$ and the α-$C_{14}H_{12}O$ crystal was random oriented. The SRS-active vibration modes of these crystals are indicated by horizontal brackets. Other notations as in Fig.1

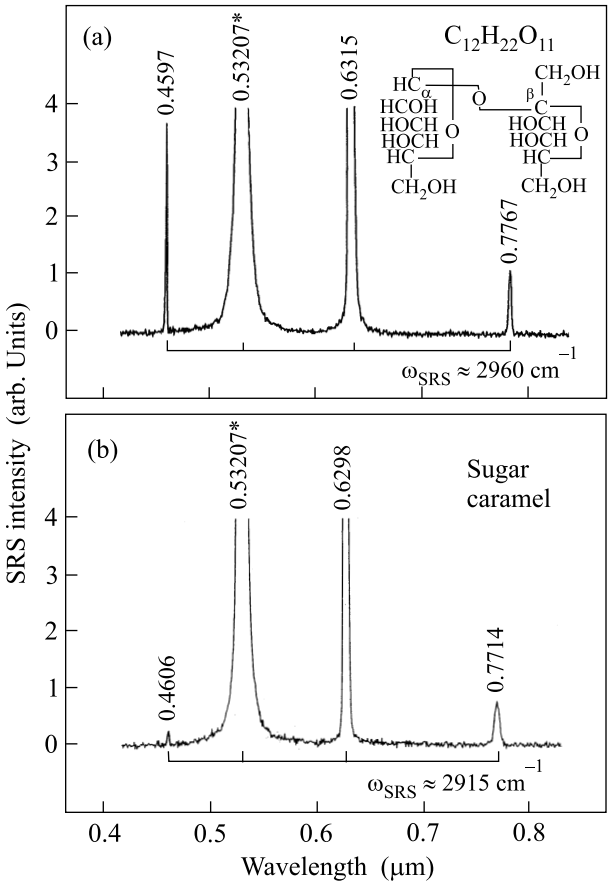

Fig.6. Random oriented Stokes and anti-Stokes lasing spectra of (a) a monoclinic $C_{12}H_{22}O_{11}$ (sugar) crystal and (b) glassy sugar caramel obtained under picosecond excitation at $\lambda_{f2} = 0.53207$ μm wavelength [21]. The SRS-active vibration modes of these organic materials are indicated by horizontal brackets. Other notations as in Fig.1

correspond to the ν(CH) vibrations of the benzene ring, ν(C = O) vibrations of the carbonyl unit, and symmetric ν(CC) vibrations of the benzene ring, respectively. The $\approx 103\,\mathrm{cm}^{-1}$ SRS-mode is lattice vibration;

4. Nonlinear laser $\chi^{(3)}$- and $\chi^{(2)}$-effects. In addition to very large Raman shift and efficient first Stokes generation in discovered SRS-active organic crystals in same an acentric of them, what are more a polar crystals, were observed combined nonlinear lasing effects, namely self-FD and self-SFM [19–21]. This potential allows to classify these materials a as promising $(\chi^{(3)} + \chi^{(2)})$-medium for a new type of laser-frequency converters.

4.1. $C_{12}H_{22}O_{11}$ (sucrose or sugar) crystal [21]. Due to its low symmetry and, hence, the large number of the vibrational modes (3NZ = 270; $\Gamma_N = 133A + 137B$, here $(A+2B)$ are acoustic modes), it is quite difficult at this initial stage of the research to establish the relation of observed SRS-mode $\omega_{SRS} \approx 2960\,\mathrm{cm}^{-1}$ (Fig.6a) to the specific C-H vibrational bond (ν[CH] or ν[CH_2]). It is interesting to note here that food sugar glassy caramel offers also very efficient SRS lasing (Fig.6b). Besides intensive Stokes and anti-Stokes lasing components, under picocesond pumping in a sugar, which is sufficiently good UV crystals, were also observed rather efficient $(\chi^{(3)}+\chi^{(2)})$-nonlinear self-frequency conversion effects, namely the self-FD ($\lambda_{\text{self-FD}} = 0.3158\,\mu$m, i.e. $1/2\lambda_{St_1}$, or $\omega_{SHG} = 2\omega_{St_1}$) and self-SFM ($\lambda_{\text{self-SFM}} = 0.2887\,\mu$m, i.e. $\Sigma\lambda_{f2}$, λ_{St_1} or $\omega_{\text{SFM}} = \omega_{f2} + \omega_{St_1}$). The SHG- and SRS-potential, availability, very low cost, and various structural modifications of a $C_{12}H_{22}O_{11}$ make this crystal quite attractive for application in modern laser physics and nonlinear optics.

Table 4

Parametric lasing effects of nonlinear $(\chi^{(3)}+\chi^{(2)})$-interaction in organic polar crystals $C_{15}H_{19}N_3O_2$ and $C_{16}H_{15}N_3O_4$ under picosecond $Nd^{3+}:Y_3Al_5O_{12}$-laser excitation at $\lambda_{f1}=1.06415\,\mu$m wavelength [17,19].

$\chi^{(3)}$ and $\chi^{(2)}$ generation component			SRS-ctive crystal vibration mode (cm^{-1} 1))
Wavelength (μm)[1)]	Line	Attribution	
$C_{15}H_{19}N_3O_2$ crystal, $l_{SRS}\approx 0.4\,$mm [2)] (Fig.7a)			
0.53207	SHG $(1/2\lambda_{f1})$	$2\omega_{f1}$	–
0.5710	$\Sigma_{f1},\lambda_{St1}$ ($\lambda_{\text{self-SFM}}$) [3)]	$\omega_{f1}+(\omega_{f1}-\omega_{SRS})$	≈ 1280
0.6160	$\Sigma\lambda_{f1},\lambda_{St2}$ ($\lambda_{\text{self-SFM}}$) 3)	$\omega_{f1}+(\omega_{f1}-2\omega_{SRS})$	≈ 1280
0.8363	ASt_2 (λ_{ASt2})	$\omega_{f1}+2\omega_{SRS}$	≈ 1280
0.9366	ASt_1 (λ_{ASt1})	$\omega_{f1}+\omega_{SRS}$	≈ 1280
1.06415	λ_{f1}	ω_{f1}	–
1.2320 [4)]	St_1 (λ_{St1})	$\omega_{f1}-\omega_{SRS}$	≈ 1280
1.4626 [4)]	St_2 (λ_{St2})	$\omega_{f1}-2\omega_{SRS}$	≈ 1280
$C_{16}H_{15}N_3O_2$ crystal, $l_{SRS}\approx 1\,$mm [2)] (Fig.7b)			
0.53207	SHG $(1/2\lambda_{f1})$	$2\omega_{f1}$	–
0.5811	$\Sigma\lambda_{f1},\lambda_{St1}$ ($\lambda_{\text{self-SFM}}$) [3)]	$\omega_{f1}+(\omega_{f1}-\omega_{SRS})$	≈ 1587
0.6402	SHG $(1/2\lambda_{St1})$	$2\omega_{St1}=2(\omega_{f1}-\omega_{SRS})$	≈ 1587
0.7126	$\Sigma\lambda_{St1},\lambda_{St2}$ ($\lambda_{\text{self-SFM}}$) [5)] $\Sigma\lambda_{f1},\lambda_{St3}$ ($\lambda_{\text{self-SFM}}$) [6)]	$(\omega_{f1}-\omega_{SRS})+(\omega_{f1}-2\omega_{SRS})$ $\omega_{f1}+(\omega_{f1}-3\omega_{SRS})$	≈ 1587
0.7955	ASt_2 $(\pi\lambda_{ASt2})$	$\omega_{f1}+2\omega_{SRS}$	≈ 1587
0.8334	SHG $(1/2\lambda_{St2})$	$2\omega_{St2}=2(\omega_{f1}-2\omega_{SRS})$	≈ 1587
0.9104	ASt_1 (λA_{St1})	$\omega_{f1}+\omega_{SRS}$	≈ 1587
1.06415	λ_{f1}	ω_{f1}	–
1.2804 [4)]	St_1 (λ_{St1})	$\omega_{f1}-\omega_{SRS}$	≈ 1587
1.6069 [4)]	St_2 (λ_{St2})	$\omega_{f1}-2\omega_{SRS}$	≈ 1587

[1)] Measurement accuracy is $\pm 0.0003\,\mu$m.
[2)] ω_{SRS} is the SRS-lasing length of crystalline element.
[3)] $\lambda_{\text{self-SFM}}$ is the wavelength of the self-sum-frequency mixing generation in which was involved the pumping with the fundamental ω_{f1} frequency and arising in the crystal first or econd Stokes lasing with $\omega_{St_1}=\omega_{f1}-\omega_{SRS}$ or $\omega_{St2}=\omega_{f1}-2\omega_{SRS}$ frequency.
[4)] Due to zero sensitivity of used Si-CCD sensor (see Fig.2) the Stokes lasing at this wavelength is not detectable.
[5)] $\lambda_{\text{self-SFM}}$ is the wavelength of the self-sum-frequency mixing generation in which was involved the pumping with the first and second Stokes lasing emissions with $\omega_{St1}=\omega_{f1}-\omega_{SRS}$ and $\omega_{St2}=\omega_{f1}-2\omega_{SRS}$ frequency.
[6)] Due to strong absorption (optical transparent of this crystal covers the spectral range of $\approx 0.51-\approx 2.2\,\mu$m, see also Fig.7b) it is possible, in general, weak third Stokes lasing at the wavelength $\lambda_{St3}=2.1570\,\mu$m, but this self-sum-frequency mixing generation process is unreal.

4.2. $C_{15}H_{19}N_3O_3$ (AANP) [19] and $C_{16}H_{15}N_3O_4$ (MNBA) [20] crystals. In these papers has been discovered a great potential for very efficient SRS acting of these two polar organic crystals. To our best knowledge, among all known $\chi^{(3)}$-active crystals they offer the greatest value of the steady-state Raman gain coefficient in near IR. These crystals are promising candidate for a new generation of Raman laser converters, where relatively short their SRS-interaction lengths (less then 1 mm) allow for miniaturization. In AANP and MNBA were observed also several new parametric lasing effects which are illustrated in Table 4 and Fig. 7. According to [19], for the 39-atomic $C_{15}H_{19}N_3O_3$ of a AANP structure overall degrees of freedom $3NZ=468$ distributed into

$$\Gamma_N = 117A_1 + 117A_2 + 117B_1 + 117B_2$$

irreducible representations. The vibration modes can be divided into acoustic $\Gamma_T = A_1 + B_1 + B_2$, internal $\Gamma_i = 111A_1 + 111A_2 + 111B_1 + 111B_2$, and translatory and rotatory $\Gamma_{T'} = 2A_1 + 3A_2 + 2B_1 + 2B_2$ and $\Gamma_R = 3A_1 + 3A_2 + 3B_1 + 3B_2$, respectively. All optical modes are Raman active. Observed SRS spectrum shows (Fig.7a) Stokes and anti-Stokes lines which related to the $\omega_{SRS}\approx 1280\,cm^{-1}$ vibration mode. It connected with strongest vibration of the bond C–N–C which links the pyridine ring and adamantylamino system of AANP crystal. Unfortunately, vibration mode analysis for a MNBA crystal is embarrassing at present due to absence of precise X-ray data. It should be done

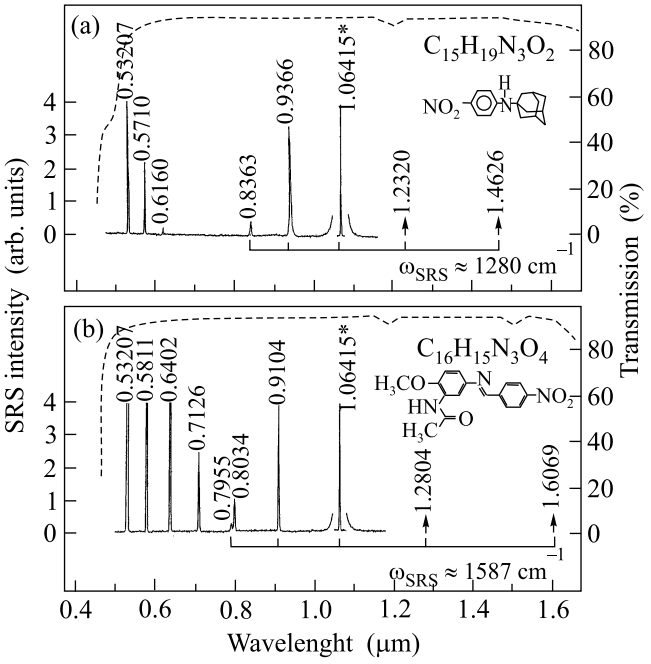

Fig.7. Parametric Raman lasing spectra of (a) orthorhombic $C_{15}H_{19}N_3O_2$ (AANP) and (b) monoclinic $C_{16}H_{15}N_3O_4$ (MNBA) crystals obtained in pumping geometry $b(aa)b$ for AANP and $b(\approx a \approx a)b$ for MNBA under picosecond excitation at $\lambda_{f1} = 1.06415\,\mu$m wavelength [17, 19]. The arrows indicate the spectral positions of the first and second Stokes lines non-detectable by the used Si-CCD sensor (see Fig.2). The fragments of nonpolarized transmission spectra of 0.4- and $\approx$ 1-mm thick samples for AANP and MNBA, respectively, are shouwn by dashed lines. The SRS-active vibration modes of these strongly nonlinear crystal are indicated by horizontal brackets. Other notations as in Fig.1

late. The large nonlinearities and hence a very efficient Stokes and anti-Stokes generation related to the $\omega_{SRS} \approx 1587\,\mathrm{cm}^{-1}$ vibration mode and other manifestation of frequency conversion lasing of MNBA with aromatic rings, donor $-OCH_3$ and acceptor group $-NHCOCH_3$, are due to extended π-electron conjugation [25, 46].

5. Conclusion. We have demonstrated a great potential for efficient SRS laser acting in several organic and organometallic crystals. These first observation of their large frequency shifts, high steady-state first Stokes Raman gain coefficients, as well as self-FD and self-SFM parametric effects let us hope that these novel materials may be used for a new generation of Raman laser converters, where relatively short their nonlinear $\chi^{(3)}$-interaction lengths allow for very attractive miniaturization. Nearly completion the paper will be in order to illustrate the results of our experimental estimations of corresponding value of the gain $g_{ssR}^{St_1}$ coefficients for several investigated crystals. These data a given in Table 5.

First of all the author obliged to note that the idea to start the SRS experiments with organic crystals was actively discussed during the 3-rd International symposium on "Modern Problems of Laser Physics" in Novosibirsk and interestedly blessed by Academician S. N. Bagayev, the chairman of this meeting. The grateful duty of the author to stress also here that the reviewed results in this paper were obtained jointly with Professors H. J. Eichler, J. Hulliger, K. Ueda, H. Klapper, E. Haussühl, T. Kaino, J. Hanuza and their teams within scientific cooperation of the Joint Open Laboratory for Laser Crystals and Precise Laser Systems. Special thanks must go to Professor A. Z. Grasyuk for numerous discussions on SRS problems, as well as for careful reading of the manuscript and comments. The author acknowledges the partial support from the Russian Foundation for Basic Research and the Ministry of Industry, Science and Technology, as well as from Alexander von Humboldt Foundation for Research Prize and from INTAS (grant # 99-01366).

Dedicated to the 60-th Anniversary of the Institute of Crystallography of the Russian Academy of Sciences.

1. J. T. Murray, R. C. Powell, and N. Peyghambrarian, J. Lumin. **66-67**, 89 (1996).
2. A. A. Kaminskii, in: *Raman Scattering – 70 Years of the Research*, Ed. V. I. Gorelik, Lebedev Physical Institute, Moscow, 1998, p. 206.
3. *Optical Materials – Special issue*, Eds. T. T. Basiev and R. C. Powell, **11**, March 1999.
4. G. A. Pasmanik, Laser Focus World **35**, 137 (1999).
5. J. Hulliger, A. A. Kaminskii, and H. J. Eichler, Adv. Funct. Mater. **11**, 243 (2001).
6. J. Barnes, in: *Proc. of the 19-th Internat. Laser Lidar Conference*, 1998, p. 619.
7. W. T. Roberts, J. T. Murray, W. L. Austin et al., Proc. SPIE **3353**, 347 (1998).
8. B. Chiao and B. P. Stoicheff, Phys. Rev. Lett. **12**, 290 (1964).
9. K. K. Lai, W. Schusslbauer, H. Silberbauer et al., Phys. Rev. **B42**, 5834 (1990).
10. S. N. Korpukhin and A. I. Stepanov, Sov. J. Quantum Electron. **16**, 1027 (1986).
11. P. Cerny, P. G. Zverev, H. Jelinkova, and T. T. Basiev, Opt. Commun. **177**, 397 (2000).
12. A. A. Kaminskii, *Crystalline Lasers: Physical Processes and Operating Schemes*, CRC Press, Boca Raton, 1996.
13. V. G. Dmitriev, G. G. Gurzadyan, and D. N. Nikogosyan, *Handbook of Nonlinear Optical Crystals*, Springer, Berlin, 1999.
14. A. A. Kaminskii, H. J. Eichler, K. Ueda et al., Appl. Opt. **38**, 4533 (1999).

Table 5

The steady-state Raman gain coefficients of Raman spectroscopic properties of organic and organometallic crystals[1)]

Crystal	First Stokes lasing characteristics				Raman spectroscopic property		
	$\lambda_{f1} = 1.06415\,\mu$m		$\lambda_{f2} = 0.53207\,\mu$m		ω_{SRS} (cm^{-1})	$\Delta\nu_R$ (cm^{-1})	T_2 (ps)
	λ_{St_1} (μm)	$g_{ssR}^{St_1}$ (cm/GW)	λ_{St_1} (μm)	$g_{ssR}^{St_1}$ (cm/GW)			
Organic							
$C_{12}H_{22}O_{11}$	–	–	0.6315	> 6.5	≈ 2960	≈ 7	≈ 2
$C_{13}H_{10}O$	1.1906	≈ 2.8	0.5619	> 10	998	≈ 3.5	≈ 3
			0.6360	> 10	3070	≈ 6.5	≈ 1.6
$C_{15}H_{19}N_3O_2$	1.2320	> 15 [2)]	–	–	≈ 1280	≈ 24 [3)]	≈ 0.44
$C_{16}H_{15}N_3O_4$	1.2804	> 14 [2)]	–	–	≈ 1587	1.5	≈ 7
Organometallic							
$C_{14}H_{26}N_8O_{13}Zr$	1.1920	≈ 3.8	0.5622	> 10	≈ 1008	≈ 5	≈ 2
	1.5487	3.2 [2)]	0.6307	> 9	≈ 2940	≈ 14 [3)]	≈ 0.8

[1)] Some of listed data are unpublished.
[2)] For this case, using nanosecond Nd^{3+}:$Y_3Al_5O_{12}$ laser ($\tau_p \approx 20$ ns) and an avalanche Ge detector we can estimated only the lower limiting value of the $g_{ssR}^{St_1}$ coefficient.
[3)] Inhomogeneously broadened line.

15. *CRC Handbook of Laser Science and Technology*, Ed. M. J. Weber, CRC Press, Boca Raton, 1986, vol. IV.
16. G. Eckhard, D. P. Bortfeld, and M. Geller, Appl. Phys. Lett. **3**, 137 (1963).
17. A. A. Kaminskii, J. Hulliger, and H. J. Eichler, Phys. Stat. Sol. **(a)186**, R19 (2001).
18. A. A. Kaminskii, H. Klapper, J. Hulliger et al., Laser Phys. **12**, 1041 (2002).
19. A. A. Kaminskii, T. Kaino, T. Taima et al., Jpn. J. Appl. Phys. **41**, L603 (2002).
20. A. A. Kaminskii, E. Haussühl, J. Hulliger et al., Phys. Stat. Sol. **(a)193**, R167 (2002).
21. A. A. Kaminskii, Crystallogr. Rep. **48**, 295 (2003).
22. H. Kutzke, M. Al-Mansour, and H. Klapper, J. Mol. Struct. **374**, 129 (1996).
23. C. J. Brown and R. Sadanga, Acta Crystallogr. **18**, 158 (1965).
24. E. Haussuhl, G. Giester, and E. Tillmanns, Z. Kristallogr. NCS **214**, 375 (1999).
25. Ch. Bosshard, K. Sutter, Ph. Pretre et al., *Organic Nonlinear Optical Materials*, Gordon and Beach, Bassel, 1995.
26. *Nonlinear Optics of Organic Molecules and Polymers*, Eds. H. S. Nolwa and S. Miyat, CRC Press, Boca Raton, 1996.
27. E. L. Woodbury and W. K. Ng, Proc. IRE **50**, 2367 (1962).
28. R. W. Boyd, *Nonlinear Optics*, Academic Press, New York, 1992.
29. Y. R. Shen, *The Principles of Nonlinear Optics*, Wiley, New York, 1984.
30. J. F. Reintjes, in: *CRC Handbook of Laser Science and Technology*, Supplement 2: *Optical Materials*, Ed. M. J. Weber, CRC Press, Boca Raton, 1995, p. 346.
31. *Nonlinear Optics*, Eds. P. G. Harper and B. S. Wherrett, Academic Press, London, 1977.
32. W. Kaiser and M. Maier, in: *Laser Handbook*, Eds. F. T. Arichi and E. O. Schulz-Dubois, North-Holland, Amsterdam, 1972, Vol. 2, p. 10077.
33. A. Laubereau, in: *Non-linear Raman Spectroscopy and its Chemical Applications*, Eds. W. Kiefer and D. A. Long, Reidel, Dorderect, 1982, p. 183.
34. N. Bloembergen, *Nonlinear Optics* Benjimin, San Diego, 1992.
35. A. Z. Grasyuk, Sov. J. Quantum Electron. **4**, 269 (1974).
36. A. A. Kaminskii, *Laser Crystals, Their Physics and Properties*, Springer, Berlin, 1981 and 1980.
37. A. Z. Grasyuk, S. B. Kurbasov, L. L. Losev et al., Quantum Electron. **28**, 162 (1998).
38. T. T. Basiev, A. A. Sobol, P. G. Zverev et al., Appl. Opt. **38**, 594 (1999).
39. M. Maier, Appl. Phys. **11**, 209 (1976).
40. D. C. Hanna, D. J. Poiner, and D. J. Pratt, IEEE J. Quantum Electron. **22**, 332 (1986).
41. P. Cerny, H. Jelinkova, T. T. Basiev, and P. G. Zverev, IEEE J. Quantum. Electron. **38**, 1471 (2002).
42. A. A. Kaminskii, S. N. Baghayev, J. Hulliger et al., Appl. Phys. **B67**, 157 (1998).
43. A. A. Kaminskii, C. L. McCray, H. R. Lee et al., Opt. Commun. **183**, 277 (2000).
44. H. J. Eichler and B. Liu, Opt. Mater. **1**, 21 (1992).
45. D. L. Rousseau, R. P. Baumann, and S. P. S. Porto, J. Raman Spectrosc. **10**, 253 (1981).
46. *Nonlinear Optics of Organic Molecules and Polymers*, Eds. H. S. Nalwa and S. Miyat, CRC Press, Boca Raton, 1996.